communications physics

A Nature Portfolio journal

Article

https://doi.org/10.1038/s42005-025-02385-7

Quantum restoration of symmetry protected topological phases

Dhruv Tiwari [1,2] ✉, Steffen Bollmann[1], Sebastian Paeckel [3] & Elio J. König [1,4]

Symmetry protected topological (SPT) phases are fundamental quantum many-body states of matter beyond Landau's paradigm. Here, we introduce the concept of quantum restoration of SPT (QRSPT) phases, where the protecting symmetry appears to be spontaneously broken at the shortest spatiotemporal scales, but restored after averaging over quantum fluctuations, so that topological features re-emerge. To illustrate the concept, we study a one-dimensional fermionic Su-Schrieffer-Heeger model with fluctuating superconducting order. We solve this problem in several limiting cases using a variety of analytical methods and compare them to numerical (density matrix renormalization group) simulations, which are valid throughout the parameter regime. We thereby map out the phase diagram and identify a QRSPT phase with topological features which are reminiscent of (but not identical to) the topology of the underlying free fermion system. The paradigm of QRSPT phases thereby stimulates a new perspective for the constructive design of novel topological quantum many-body phases.

Symmetries play an exceptional role in characterizing quantum materials. On the one hand, following Landau's legacy[1], spontaneous symmetry breaking (SSB) has been of paramount importance for classifying many-body ground states. More recent advances demonstrate that, even when symmetry-breaking order parameters form locally, strong quantum fluctuations of their orientation may impede true SSB and give way to exotic phenomena such as vestigial order[2,3] and quantum paramagnetism such as quantum spin liquids[4] – a mechanism sometimes called "quantum restoration" of symmetry[5–8]. On the other hand, symmetries are also of paramount importance for characterizing order beyond the Landau paradigm. Specifically, a given Symmetry Protected Topological (SPT) phase[9–11] represents a class of gapped short-range entangled many-body quantum states that cannot be connected adiabatically to a different SPT phase as long as the symmetry is unbroken[12]. Amongst the most glaring properties that are robust to symmetry-preserving perturbations are protected gapless boundary excitations in the presence of non-trivial SPT order.

Classic examples of states exhibiting non-trivial SPT order are free fermion topological insulators[13] and the bosonic, strongly correlated "Haldane" phase of antiferromagnetic spin-1 chains[14,15]. There exist multiple theoretical and numerical ways of characterizing and detecting phases (or classes) of SPT order[12,16–23]. In particular, the classification of interacting SPT phases (for a given symmetry group) can be different from their non-interacting counterpart[24–26].

Of particular interest for the present work are SPT phases where the protecting symmetry is present only on average. The historically first example regards disordered systems where the symmetry may be broken in each realization, but restored upon ensemble average[27–32]. In mathematical terms, consider disorder fields ϕ with a probability distribution $\mathcal{P}[\phi]$, which is invariant under the protecting symmetry. Then, the effective Euclidean action of replicated matter fields ψ_r

$$S_{\text{eff}}[\{\psi_r\}] = -\ln\left(\int \mathcal{D}\phi\mathcal{P}[\phi]\exp\left\{-\sum_r S_0[\psi_r,\phi]\right\}\right), \qquad (1)$$

may display features of an SPT phase even if $S_0[\psi_r, \phi]$ for a given configuration ϕ breaks the protecting symmetry. Recent advances generalize the concept of such average SPT phases to amorphous systems[33] and open quantum systems with decoherence and mixed quantum states[34].

In this paper, we introduce the concept of quantum restoration of symmetry protected topological (QRSPT) phases: They occur in failed SSB states where strong quantum fluctuations of the local order parameter orientation lead to restoration of a symmetry protecting an SPT phase. Subsequently, the main part of the paper is devoted to an exemplary model, a spinful Su-Schrieffer-Heeger model with fluctuating s-wave super-

[1]Max-Planck Institute for Solid State Research, Stuttgart, Germany. [2]Max Planck Institute for the Physics of Complex Systems, Dresden, Germany. [3]Department of Physics, Arnold Sommerfeld Center for Theoretical Physics (ASC), Munich Center for Quantum Science and Technology (MCQST), Ludwig-Maximilians-Universität München, München, Germany. [4]Department of Physics, University of Wisconsin-Madison, Madison, WI, USA. ✉e-mail: tiwari@pks.mpg.de

conductivity (see Eq. (3)), displaying the outlined general phenomenology. We have obtained the phase diagram of this model using various analytical and numerical techniques. The QRSPT phase obtained for this model confirms the above-mentioned idea of how quantum fluctuations can restore the symmetries in certain regimes.

Results and Discussions

Quantum restoration of SPT phases

For an illustration of the general QRSPT paradigm, see Fig. 1. First, concentrate on a clean, free fermion topological insulator or superconductor with symmetry group G. Unitary symmetries allow to block diagonalize the Bloch Hamiltonian, each block being subsequently topologically scrutinized by the tenfold-way methodology[35]. In particular, we consider the case where the topological invariants in the various blocks are non-zero but sum up to zero. Importantly, the protecting symmetry ensures different quantum numbers for zero boundary states emanating from different blocks, precluding any mutual annihilation.

Next, Fig. 1b), we include interactions and assume that a finite order parameter amplitude develops such that the symmetry which ensures the block-diagonalization of the Hamiltonian appears to be spontaneously broken. At the level of a static mean-field order parameter, one may still resort to non-interacting band topology but the Bloch Hamiltonian can no longer be block diagonalized. It must thus be treated as a whole, and the topological invariant vanishes.

The formation of mean-field order parameters is insufficient to demonstrate actual SSB. In particular, for continuous groups G, quantum fluctuations of the orientation of the order parameter ("Goldstone modes" ϕ) may inhibit true long-range order. In this case, at the longest time/length scales G symmetry is recovered and can lead to quantum restoration of SPT phenomenology, Fig. 1c). In mathematical terms, the effective Euclidean action of fermions ψ

$$S_{\text{eff}}[\psi] = -\ln\left(\int \mathcal{D}\phi\, \exp\{-S[\psi,\phi] - S_{\text{Goldstone}}[\phi]\}\right), \tag{2}$$

displays features of a SPT phase, even though a given order parameter field configuration ϕ breaks the protecting symmetry G at each instance of imaginary time.

We conclude this section with a few comments. First, the difference between the average over static disorder in Eq. (1), and the average over Goldstone modes in Eq. (2) is the appearance of temporal correlations. These are a consequence of Ehrenfest's theorem, which ties real-time quantum fluctuations of the observable ϕ to their commutator with the Hamiltonian (one may equally well represent Eq. (2) in the Wick-rotated real-time field integral). Second, the reader may question the physical relevance of the intermediate technical step, Fig. 1b), which introduces a static symmetry-breaking order parameter. On the one hand, the two-step logic may reflect theoretical approaches in which, first a mean-field solution is searched and subsequently fluctuations are included. It is valid in situations that are particularly relevant to low dimensions, where the coherence length/time scales of quantum restoration may be exponentially larger than spatiotemporal scales suggested by mean-field physics. On the other hand, independently of any methodology, the QRSPT phases explain how SPT states emerge near SSB, e.g., how the blue SPT phase emerges out of the green superconductor in Fig. 2c). Third, in the above, we discussed the situation of intrinsic SSB within the topological fermionic system. In one and two dimensions, it is equally conceivable that the fluctuating order parameter and the Goldstone modes ϕ emanate from proximitizing the G-symmetric fermionic material with a second material with spontaneous symmetry breaking (e.g., a magnet or superfluid). Such a heterostructure also represents bona-fide implementation of two-fluid models of the type of Eq. (2). Fourth, we highlight that the interplay of Dirac electrons with quantum disordered order parameters, in particular through condensation of topological defects, has been discussed in the past, particularly in connection with interacting topological insulator boundary states[7] and with the paradigm of symmetric mass generation[8]. Fifth, one may wonder what happens to the system if the quantum fluctuations are weak and the true long-range order is established. Per Goldstone's theorem, the bulk system is gapless, yet it is possible that the underlying free fermion topology enforces the emergence of additional topological terms in the action describing order parameter fluctuations[36,37], leading potentially to topological Goldstone phases of matter[38]. Finally, one may argue that $S_{\text{eff}}[\psi]$ is nothing but a model for a very specific interacting fermionic SPT phase[20,39,40], in particular when ϕ correlations are short-range deep in the quantum disordered state, so that $S_{\text{eff}}[\psi]$ describes a local theory. While this statement is in principle true, the model scrutinized in this paper demonstrates that the paradigm of QRSPT phases promises much richer physics, in particular near the phase transitions of the system, where fermions and Goldstone bosons mutually stabilize the physics of long-range interacting quantum systems[41] (the classic solid state example is RKKY[42–44] interactions).

Model

As a paradigmatic model to illustrate the concept of QRSPT phases, we study a mesoscopic topological Josephson junction array. We assume fermionic quantum dots forming a spinful Su-Schrieffer-Heeger (SSH)[45,46] chain, Fig. 2a) and couple it to an array of floating superconducting islands[47] as follows

$$\begin{aligned}\hat{H} = {} & E_C \sum_X (2\hat{N}_X + \hat{n}_X - N_g)^2 \\ & - \sum_{X,\sigma} (t\, d^\dagger_{X,A,\sigma} d_{X,B,\sigma} + t'\, d^\dagger_{X+1,A,\sigma} d_{X,B,\sigma} + \text{H.c.}) \\ & - \frac{\Delta}{2} \sum_{X,j,\sigma,\sigma'} (e^{-i\hat{\phi}_X} d^\dagger_{X,j,\sigma} [\sigma_y]_{\sigma,\sigma'} d^\dagger_{X,j,\sigma'} + \text{H.c.}),\end{aligned} \tag{3}$$

where $X \in \mathbb{Z}, j \in \{A,B\}$ and $\sigma \in \{\uparrow,\downarrow\}$ denote the unit cell, sublattice of SSH chain and the spin, respectively. The operator $\hat{N}_X = -i\partial_{\phi_X}$ measures the number of Cooper-pairs at the Xth Cooper-pair box and is conjugate to the Cooper-pair annihilator $e^{-i\hat{\phi}_X}$ (i.e. to the fluctuating superconducting order parameter). Similarly $\hat{n}_X = \sum_{j,\sigma} d^\dagger_{X,j,\sigma} d_{X,j,\sigma}$ measures the number of electrons in the unit cell X. We denote the unit cell using the uppercase

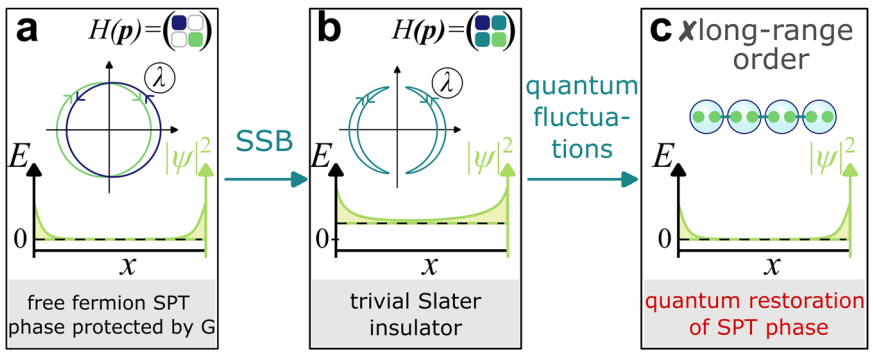

Fig. 1 | Illustration of the quantum restoration of a symmetry protected topological phase. a Consider a free fermion symmetry protected topological (SPT) phase where the symmetry group G prevents the admixture of distinct topological sectors of the Bloch Hamiltonian and of zero-energy boundary states with distinct quantum numbers. **b** Spontaneous symmetry breaking (SSB) of G trivializes the free fermion topology, but **c** strong quantum fluctuations of the order parameter may destroy long-range order even if the local expectation value of the order parameter amplitude is non-zero. Thereby, topological features reemerge, and the SPT phase is quantum restored.

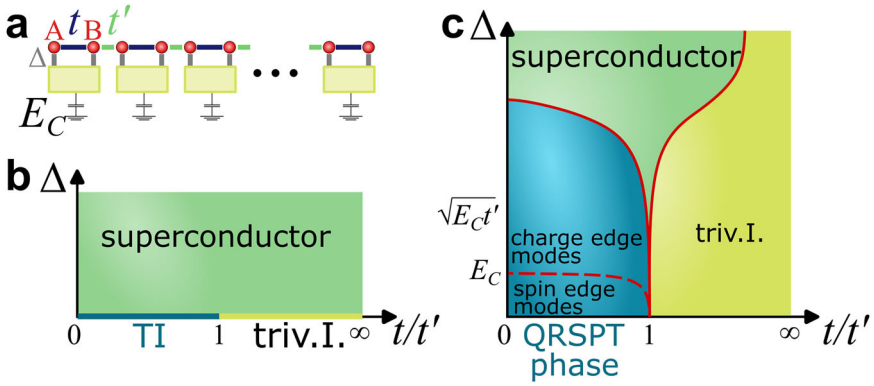

Fig. 2 | Schematic representation of the model and the phase diagram at the mean field level and beyond. a Schematic representation of the model, Eq. (3). The rectangular boxes denote the Cooper pair boxes. **b** Phase diagram of the Bogoliubov-de Gennes free-fermion Hamiltonian, Eq. (4): Δ breaks the symmetry protecting the free-fermion topology (cf Fig. 1b) so that topological and trivial phases may be adiabatically connected. TI and triv.I. represent topological and trivial insulator respectively. Note that there is a gap closure (as expected from standard SSH physics) at $t = t'$ (for $\Delta = 0$). **c** Schematic phase diagram of Eq. (3). Note the region exhibiting quantum restoration of symmetry protected topological (QRSPT) phase appears at small Δ and $t < t'$.

index X, whereas the lowercase index x represents the continuum position variable (appears later in the paper). Note that the proximity-induced coupling strength Δ is much smaller than the bulk superconducting gap; this allows to ignore the quasiparticle states within the superconductor for physical considerations limited to the lowest energy excitations of the model. We also assume that the dimensions of the superconductor are much larger than the coherence length of the Cooper-pairs, which allows us to neglect crossed Andreev reflection[47–49]. For simplicity, we set the Josephson coupling between the superconducting islands to be zero. We restrict ourselves to $E_C < \sqrt{t^2 + t'^2}$ (since our analytical calculations are only valid in this regime) and even values of the gate voltage N_g. The basic symmetries of Eq. (3) are the conservation of total charge $\sum_X 2\hat{N}_X + \hat{n}_X$ ($U(1)$ symmetry) and a combined sublattice and particle-hole transformation denoted by C, see methods and supplementary note 1.

We first elucidate in which sense Eq. (3) displays QRSPT phenomenology. At $\Delta = E_C = 0$, the fermionic sector decouples from bosons and displays standard SSH topology. Next, we include superconductivity. A static mean-field approximation corresponds to $E_C = 0$ such that the superconducting phase at each island becomes a classical variable which we gauge to $\phi_X = 0$, throughout. The Bloch Hamiltonian in Nambu space

$$H(p) = \begin{pmatrix} 0 & D(p) \\ D^\dagger(p) & 0 \end{pmatrix}, \tag{4a}$$

$$D(p) = \begin{pmatrix} -(t + t' e^{ip}) & i\Delta \\ -i\Delta & (t + t' e^{-ip}) \end{pmatrix}, \tag{4b}$$

ceases to be block diagonal in the presence of Δ ($U(1)$ and C symmetry breaking) term, thereby losing the compensated topology of electron and hole bands, cf. the loss of winding numbers of $D(p)$ illustrated in Fig. 1a) vs. b). Note that commonly Bardeen-Cooper-Schrieffer (BCS) trial states are not regarded as Slater determinants. However, using the combination of spin-selective particle-hole symmetry and unitary (Bogoliubov) transformation, they can be manifestly written as a Slater determinant[50]. Thus, we have used the term trivial Slater insulator for trivial BCS states as well. The model is gapped for all non-zero values of Δ, Fig. 2b), thus allowing for an adiabatic connection of the topological phase of the SSH model (at $\Delta = 0, t < t'$) to the trivial phase (at $\Delta = 0, t > t'$). Simultaneously, the edge spectrum of the SSH model in the presence of static, homogenous Δ is gapped out as the spinful fermionic edge states combine into Cooper pairs.

Physics beyond the semiclassical short-range order is introduced by Coulomb interactions (represented by E_C term) which, by Ehrenfest's theorem, leads to quantum fluctuations of the phase.

The phase diagram (schematically shown in Fig. 2c), contains a QRSPT phase at small Δ and $t < t'$, a superconductor emanating from the free fermion critical point $\Delta = 0, t = t'$ and a trivial gapped phase for $t > t'$ and small Δ. Leaving details to the remainder of the paper, we now summarize the pecularities of these phases. Most importantly, the QRSPT phase is characterized by edge states even for non-zero values of Δ as derived by perturbing the system around an integrable limit at $t \ll t'$ and by analyzing soliton solutions of the field theory near $t = t'$. A particular curiosity of the present model is the boundary transition from spin to charge edge modes within the QRSPT which is also confirmed numerically. Additionally, the topological nature is corroborated by symmetry fractionalization arguments and, numerically, by the observation of degeneracies in the entanglement spectrum. Contrary to the implications of Eq. (4), we observe –both in analytical field theory and DMRG (Density matrix renormalization group)– a phase transition (or intermediate phase) near $t = t'$ for non-zero values of Δ. It separates the topological phase from a trivial phase without edge states or degeneracies in the entanglement spectrum. The critical point serves as a seed for a superconducting phase at large Δ, which is stabilized by emergent Josephson coupling between the islands.

Perturbation about the dimerized limits

We first study the effect of introducing Δ and E_C perturbatively about the two extreme regimes corresponding to $t = 0$ and $t' = 0$ assuming $\Delta, E_C \ll \sqrt{t^2 + t'^2}$. In the former regime, contrary to Eq. (4) we do observe a gapless edge spectrum (accompanied by a peculiar boundary transition from gapless spin edge modes to gapless charge edge modes) for $\Delta \neq 0$ as discussed below. For $t = 0$ ($\Delta, E_C = 0$), the SSH model is in its topological state with intercell dimers. Assuming periodic boundary conditions, the groundstate of the SSH model in this regime is given by:

$$\begin{aligned} |\psi(\{N_X\})\rangle &= \prod_{X=1}^{N} |N_X\rangle \otimes |\psi_{\mathrm{SSH}}\rangle, \\ |\psi_{\mathrm{SSH}}\rangle &= \left[\prod_{X=1}^{N} \left(\frac{d^\dagger_{A,X,\uparrow} + d^\dagger_{B,X+1,\uparrow}}{\sqrt{2}}\right)\left(\frac{d^\dagger_{A,X,\downarrow} + d^\dagger_{B,X+1,\downarrow}}{\sqrt{2}}\right)\right]|0\rangle, \end{aligned} \tag{5}$$

where N is the number of unit cells and $|0\rangle$ is the vacuum state. Note that the number N_X of bosons in each cell is arbitrary in Eq. (5) since the terms E_C and Δ are zero implying no coupling of bosons and fermions. This massive degeneracy is lifted upon introducing E_C as a perturbation (Δ induced matrix elements within the ground state manifold vanish) so that the correction to groundstate energy is positive and extensive in E_C up to first orders in Δ and E_C. The average fermion occupation of two in $|\psi_{\mathrm{SSH}}\rangle$ implies that the groundstate corresponds to Eq. (5) with $N_X = N_g - 2$ ($N_g \in 2\mathbb{Z}$), see supplementary note 2 for details (we choose $N_g = 2$ henceforth).

To study the edge states of this model in this regime, we transform to open boundary conditions (OBC) by assuming that the state $|\psi_0\rangle = |\psi(\{N_X = 0\})\rangle$ still describes the ground state under OBC except for the first and last Cooper-pair box and fermionic site. Thus, the effective edge Hamiltonian is given by:

$$\langle\psi_0|\hat{H}|\psi_0\rangle = \hat{H}_{\mathrm{left-edge}} + \hat{H}_{\mathrm{right-edge}} + E_{\mathrm{bulk}}, \tag{6}$$

where E_{bulk} corresponds to the energy of the state $|\psi_0\rangle$ in the bulk. The effective edge Hamiltonian on the left edge is given by:

$$\hat{H}_{\text{left-edge}} = E_C(2\hat{N}_1 + \hat{n}_{A,1} - 1)^2 - \frac{\Delta}{2}(e^{-i\hat{\phi}_1} d^\dagger_{1,A}\sigma_y d^\dagger_{1,A} + \text{H.c.}) + \frac{E_C}{2}. \tag{7}$$

This edge-Hamiltonian can be readily solved; the lowest energy edge excitations as a function of Δ are plotted in Fig. 3(a). Analogous results hold at the right edge. While the ground state is always degenerate, an edge transition from gapless spin edge modes to gapless charge edge modes at $\Delta = E_C$ occurs.

We use techniques of symmetry fractionalization[16,18,51] to demonstrate that both the spin and charge edge modes are protected at least by the antiunitary particle-hole symmetry C, see supplementary note 2 for details. This antiunitary symmetry, which squares to unity in the bulk, fractionalizes at low energies into operators which act locally on the edge states. As the fractionalized representation squares to -1, it implies that C protects edge degeneracy by a generalized Kramers theorem. Thus, contrary to the case of Eq. (4), there exists an SPT phase for non-zero values of Δ. When a similar perturbative calculation is performed near $t' = 0$, the edge spectrum is gapped throughout, indicating a trivial phase, and no correction to the ground-state energy occurs to first orders in Δ and E_C. The latter result highlights the fact that our model is asymmetrical upon an exchange of t and t', see the schematic phase diagram shown in Fig. 2c).

Field theory near the free fermion critical point

We now turn to study signatures of the bulk phase transition for non-zero values of Δ and concentrate on the limit $\Delta \ll E_C$ and $|t - t'| \ll E_C \ll \sqrt{t^2 + t'^2}$.

For the unperturbed Hamiltonian (corresponding to $\Delta = 0$ in Eq. (3)), the fermionic gap is controlled by the term $|t - t'|$ (the mass gap in the SSH model), and the bosonic gap is controlled by the term E_C. Thus, bosons are fast as compared to fermions and can be integrated out to obtain an effective low-energy theory of interacting fermions, see supplementary note 3. The value of $\sqrt{t^2 + t'^2}$ serves as an estimate for the bandwidth of the single particle spectrum of free fermions (corresponding to $\Delta = E_C = 0$) and the assumption of $E_C \ll \sqrt{t^2 + t'^2}$ controls the bosonization approach on top of the linearized fermionic Hamiltonian. Its bosonized representation is given by the following action:

$$S = \sum_{\alpha=s,\rho} \int_{x,\tau} \frac{1}{4\pi K_\alpha}\left(\frac{(\partial_\tau \Phi_\alpha)^2}{u_\alpha} + (\partial_x \Phi_\alpha)^2 u_\alpha\right) - \int_{x,\tau} [G_s \cos(2\Phi_s) + M \cos(\Phi_s)\cos(\Phi_\rho)], \tag{8}$$

where s and ρ denote the spin and charge degrees of freedom, respectively and $\Phi_{\rho,s} \equiv \Phi_{\rho,s}(x,\tau)$ are bosonic fields in the corresponding sector. In terms of parameters of Eq. (3), $G_s \sim \Delta^2/(E_C a)$, $M \sim (t' - t)/a$ while Luttinger parameters $K_{\rho,s}$, and hydrodynamic velocities $u_{\rho,s}$ are contained in the methods section. To study the phase diagram of the effective action in Eq. (8), we perform a perturbative Renormalization Group (RG)[52] analysis of the bosonized action in Eq. (8) (about the fixed point of Luttinger liquid theory for both the charge and spin sector, and up to first order in prefactors of cosines). The flow equations are

$$\frac{dG_s}{dl} = (2 - 2K_s)G_s, \quad \frac{dM}{dl} = \left(2 - \frac{K_s}{2} - \frac{K_\rho}{2}\right)M, \tag{9}$$

where $l = \ln(\Lambda/\Lambda')$ and Λ (Λ') is the momentum cutoff of the theory (the running momentum cutoff). Note that in the present theory $K_s < 1$, hence the G_s term is always relevant and the system displays a spin gap for any non-zero Δ. In contrast, $K_\rho > 1$ is possible and the mass term changes from relevant (displayed in Fig. 3c)) to irrelevant (not shown) when $K_\rho + K_s = 4$ which corresponds to $\Delta \sim \sqrt{E_C t'}$ in terms of microscopic parameters entering Eq. (3).

This leads to the phase diagram illustrated in Fig. 2c): For $\Delta \ll \sqrt{E_C t'}$, non-zero M flow to a fully gapped and topologically trivial (non-trivial) insulator, the two phases being divided by a critical line. In contrast, for

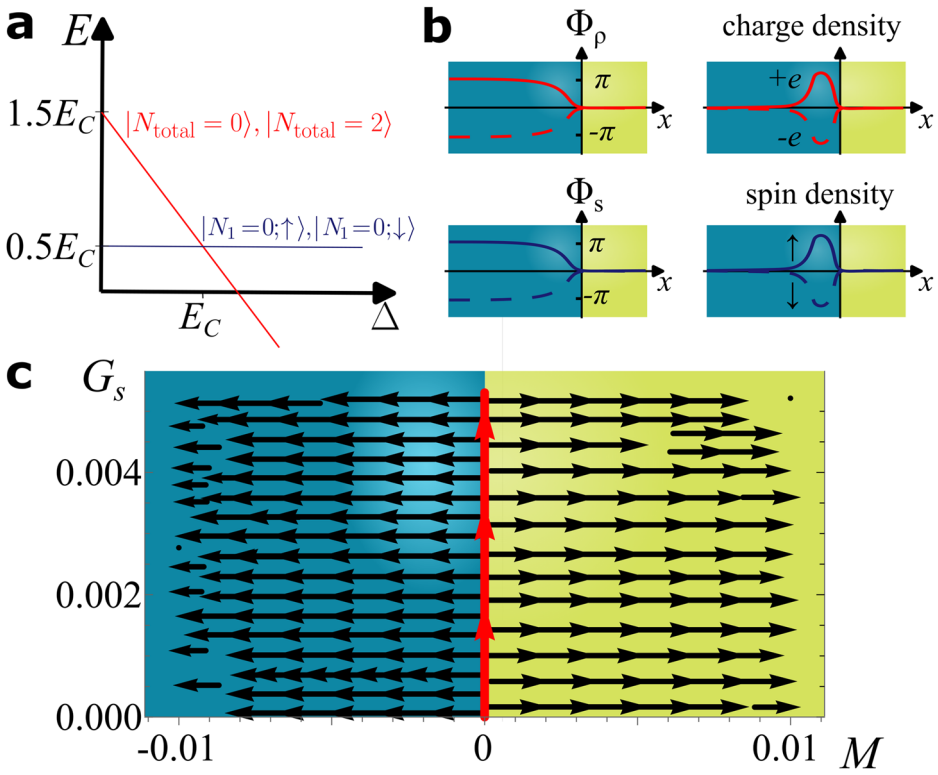

Fig. 3 | Edge transition and the renormlization group flow. a Eigenvalues of the edge Hamiltonian, Eq. (7), as a function of Δ for $t = 0$, $N_g = 2$. Note the edge transition from gapless spin edge modes to gapless charge edge modes at $\Delta = E_C$. N_1 represents the number of bosons on the first bosonic site. $N_{\text{total}} = 2N_1 + n_1$ represents the total charge on the left edge. **b** Edge states correspond to kink-like field configurations within the effective field theory near the free fermion critical point, Eq. (8). The blue and yellow regions are used to distinguish the trivial and topological insulating regimes. $\Phi_{\rho/s}$ stand for the bosonic fields corresponding to charge (red curve) and spin (blue curve) degrees of freedom, respectively. The charge (red curve) and spin (blue curve) densities, Eq. (11) and Eq. (12), exhibit the localization of respective densities close to the boundary of the trivial and non-trivial insulating states, which is the character of edge states. **c** Renormalization Group (RG) flow obtained using the flow equations given in Eq. (9). The black arrows represent flow towards an insulating state, whereas the red arrows represent flow towards a state without a charge gap.

$\Delta \gg \sqrt{E_C t'}$ one expects that the insulating phases are separated by a third phase without a charge gap. Note that this requires pushing the field theory discussed in this section beyond its limits of applicability; hence, we prove this claim later by complementary means. Importantly, unlike the case depicted in Fig. 2b), a critical theory without a charge gap separates the two insulating phases even for non-zero values of Δ. This gapless state corresponds to a singlet s-wave superconductor as it has dominant correlations of the type $e^{-i\frac{\Theta_\rho}{\sqrt{2\pi}}}\cos(\Phi_s)$[53,54] where Θ_ρ is the bosonic field conjugate to Φ_ρ.

We also studied edge modes at the interface of the phases corresponding to negative and positive values of M using semiclassics (see supplementary Note 3). Taking into account the periodicity of the bosonic variables Φ_ρ and Φ_s, the ground state in terms of the bosonic variables for $M > 0$ corresponds to $(\Phi_{\rho,f}, \Phi_{s,f}) = (0, 0)$. For $M < 0$, the groundstate corresponds to four possible values of the bosonic variables given by:

$$(\Phi_{\rho,f}, \Phi_{s,f}) = (\pm\pi, 0), (0, \pm\pi), \tag{10}$$

where these different configurations of $(\Phi_{\rho,f}, \Phi_{s,f})$ lead to the same groundstate energy in the bulk, but they imply four different edge states represented by half-kink or half-antikink in spin or charge sector, see Fig. 3b). A spin mode leads to an accumulation of spin 1/2 at the edge, which can be seen by calculating the corresponding S_z magnetization:

$$S_z = \frac{1}{2\pi}\int dx \partial_x \Phi_s = \pm\frac{1}{2}. \tag{11}$$

Similarly, charge modes lead to an edge accumulation of charge

$$N_e = \frac{e}{\pi}\int dx \partial_x \Phi_\rho = \pm e, \tag{12}$$

relative to the ground state charge configuration. We analytically determine (see supplementary note 3) the kink energies, demonstrating that the charge and spin kinks are each two-fold degenerate. Comparing those energies at non-zero Δ, we find that the ground states within this effective continuum model feature spin (charge) edge states for small (large) $\Delta < \Delta_c$ ($\Delta > \Delta_c$) with a non-analytic edge transition curve:

$$\Delta_c \simeq \sqrt{-\frac{0.177715\, W(-\alpha \log(|\delta\theta|))}{\log(|\delta\theta|)}}, \tag{13}$$

where $\delta\theta \simeq \frac{t-t'}{\sqrt{t^2+t'^2}}$, W represents Lambert's W function and $\alpha = 0.000034$. This curve is schematically shown in Fig. 2c), see supplementary note 3 for more details. Far away from the bulk transition $\frac{t}{t'} \ll 1$, the same formalism yields an edge transition at $\Delta \simeq E_C$, consistent with the edge transition obtained from perturbation theory above.

Field theory around the superconducting phase

In the regime $E_C < \Delta, |t - t'|$, the upper bound on the bosonic gap is controlled by the term E_C and is much smaller than the fermionic gap controlled by the term Δ and $|t - t'|$. Thus, we can integrate out the fermions in this regime and obtain a low-energy effective theory of bosons. Around the regime where the bosons become gapless, the effective bosonic theory can be described by a Luttinger liquid, and we determine the corresponding Luttinger liquid parameters. The procedure of integrating out fermions is non-trivial for the total Hamiltonian in Eq. (3) due to the presence of the electron density $\hat{n}_X$ in the E_C term. To make the procedure relatively simpler and transparent, it is useful to perform a basis change to a basis where fermionic fields effectively follow the slowly fluctuating superconducting phase. The bosonic action obtained after integrating out fermions is given by

$$S_{\text{eff}}(\phi) = \frac{1}{2K_{\text{SC}}}\int_{x,\tau} \frac{(\partial_\tau \phi)^2}{u_{\text{SC}}} + u_{\text{SC}}(\partial_x \phi)^2. \tag{14}$$

The main steps in the process of integrating out fermions and the definition of K_{SC} and u_{SC} in terms of model parameters are given in the methods section and supplementary note 4. K_{SC} denotes the inverse superconducting stiffness, and a phase transition from the insulating regime to a superconducting regime occurs at $K_{\text{SC}} = 1$. Note that this transition from the insulator to the superconductor is the Berezinskii-Kosterlitz-Thouless transition[55] and corresponds to the proliferation of phase slips. This condition and the expression K_{SC} in terms of microscopic parameters determine the phase boundaries plotted in red in Fig. 4a) (no fitting involved). On the side, we remark that within the effective Luttinger liquid

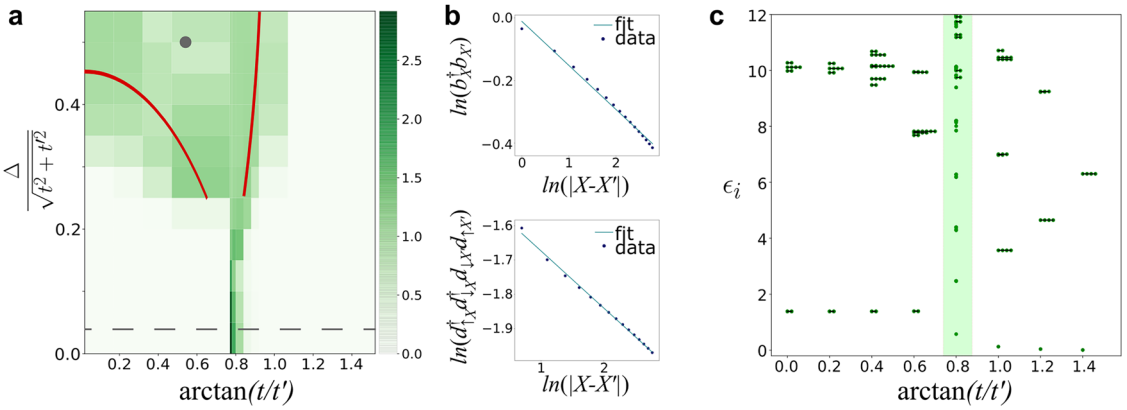

Fig. 4 | Numerical phase diagram, correlators and entanglement spectrum. **a** Color plot of the central charge obtained using finite DMRG for a system size of 40 and $N_g = 4$. The phase diagram is obtained for $\frac{E_C}{\sqrt{t^2+t'^2}} = 0.01$. Red lines denote the analytically obtained position of the Berezinskii-Kosterlitz-Thouless transition line. The grey dot (grey dashed line) correspond to the locations in parameter space at which the data in **b** and **c** are taken. **b** Log-Log plot of the bosonic and fermionic correlator for $\Delta = 50E_C$ and $\arctan(\frac{t}{t'}) = 0.47$. The power-law fit for the bosonic and fermionic correlator gives a K_{SC} value of 0.89 ± 0.01 and 1.04 ± 0.01 respectively while the analytical value of K_{SC} at this point in the phase diagram corresponds to 0.84 (see supplementary note 5 for details). The linear fit on the log-log scale indicates off-diagonal superconducting correlations as also expected from our analytical study of the phase diagram. **c** Entanglement spectrum obtained using iDMRG for $\Delta = 4E_C$ and $\frac{E_C}{\sqrt{t^2+t'^2}} = 0.01$ and $N_g = 2$. The green-shaded regime corresponds to criticality. Consistent with analytical expectations, we observe even degeneracy throughout the regime corresponding to quantum restoration of symmetry protected topological (QRSPT) phase in Fig. 2c. Note that we only show the entanglement spectrum values upto $\epsilon_i = 12$.

theory, the superconducting regime is not observed for $\frac{E_C}{\sqrt{t^2+t'^2}} > 0.02$, which could signal Mott localization throughout.

DMRG results

To model the Hamiltonian in Eq. (3) numerically, we truncate the local Hilbert space dimension of Cooper pairs (created/annihilated by $e^{\pm i\hat{\phi}_X}$) to a finite value of 8 (we observed that choosing a value as small as 4 did not affect the overall phase diagram). We used the finite and infinite Density Matrix Renormalization Group (DMRG and iDMRG, respectively) algorithms to study various features of our model. All numerical calculations were performed using the TeNPY library[56].

The phase diagram obtained using DMRG is shown in Fig. 4a) and the relevant correlation function plot in the critical phase is shown in Fig. 4b). Overall, the numerically observed phase diagram corroborates the analytical results: The Berezinskii-Kosterlitz-Thouless transition line out of the superconducting phase (red) as obtained from Eq. (14) (corresponding to $K_{SC} = 1$) captures well the boundary of the area where the central charge is $c = 1$. The correlators (given by $\langle d^\dagger_{X,\uparrow} d^\dagger_{X,\downarrow} d_{X',\downarrow} d_{X',\uparrow}\rangle$ and $\langle b^\dagger_X b_{X'}\rangle$) inside the regime with $c = 1$ are consistent with off-diagonal long-range order of a singlet superconductor, Fig. 4b). As expected, for $\Delta < \sqrt{E_C t'} \approx 0.1\sqrt{t^2+t'^2}$, the wide superconducting phase narrows to a sharp line located at $t = t'$, cf. Fig. 2c) and 4a). Finally, the nature of the insulating ($c = 0$) phases is verified using iDMRG, by means of which we obtained the entanglement spectrum of the system, see Fig. 4c). We observe an even degeneracy of all levels throughout the entanglement spectrum in the regime corresponding to the topological insulator in Fig. 2c), but not in the topologically trivial regime. Since even degeneracies are a signature of SPT order[17], this supports our analytical result of QRSPT order in our model. We also observed a similar entanglement spectrum for $N_g = 2$ as well. We also observe (see supplementary note 5) edge states by measuring local charge and spin expectation values of the DMRG ground state and an edge phase transition analogous to Fig. 3a).

Contrary to the analytical expectation, the numerically obtained central charge continuously reaches three at $t = t'$ as Δ is decreased. We attribute this observation to numerical limitations. Non-integer central charge values are not to be expected in the present context. A discussion of numerical limitations in terms of the energy variance of the obtained groundstates in the regime of large c as well as the error bars of Fig. 4c) are relegated to supplementary note 5.

Although the numerical observation of both charge and spin edge modes is consistent with C being the protecting symmetry, we observe that breaking only the C symmetry (by adding a symmetry-breaking perturbation) does not lift the degeneracies in the entanglement spectrum. This possibly implies the existence of other symmetries protecting the SPT phase, and/or it is even possible that the symmetry arguments are modified due to the presence of bosonic degrees of freedom in our model since the existing theoretical arguments are valid, for C being the protecting symmetry, only for non-interacting/interacting fermionic systems[57]. However, the degeneracies are lifted in the presence of a term that breaks total charge ($U(1)$) symmetry implying that $U(1)$ has a non trivial representation at the edge – which is not expected on general theoretical grounds[58]. At the same time, it is known that the topological classification changes from $\mathbb{Z}_4$ (for $U(1) \times C$) to $\mathbb{Z}_8$ (for C)[57]. Thus, this indirectly implies that $U(1)$ symmetry can play a role in topological characteristics of our model. Further details regarding the symmetry-breaking perturbations can be found in supplementary note 5 and we leave a detailed numerical/analytical study to characterize relevant symmetries for future works.

Conclusion

In summary, we have introduced the concept of quantum restoration of symmetry-protected topological phases, i.e. topological systems in which the underlying protecting symmetry is broken at each instance of time, but restored upon time average. To illustrate this concept, we carefully studied an interacting one-dimensional model corresponding to a spinful Su-Schrieffer-Heeger model with fluctuating superconductivity. Using combined analytical and numerical methods, we demonstrate that the features of the SPT phase are restored. It is worthwhile to highlight a phase diagram that is distinct from and arguably richer than purely fermionic interacting SSH-chains[59–65], both in terms of phases and phase transitions in the bulk and of those at the boundary. While it is generally expected that insulating QRSPT phases are related to topological zeros in the fermionic Green's function[39,66–70], we leave this as an open question for future studies along with, first, which QRSPT phases can be expected based on a given underlying free fermion SPT phase, second, whether there are universal patterns in the corresponding phase diagram between QRSPT phase and trivial phase, third, a careful analysis in higher dimensions, and fourth, robustness of QRSPT states to weak disorder. We also hope that our work will motivate the design of new physical models exhibiting SPT features by exploring the role of quantum fluctuations.

Methods

Symmetries

The model in Eq. (3) has $U(1)$ symmetry (corresponding to a conserved total charge $\sum_X 2\hat{N}_X + \hat{n}_X$) and combined sublattice and particle-hole symmetry (in the second quantization language) C given by:

$$\begin{aligned} Cd^\dagger_{X,A,\sigma}C^{-1} &= d_{X,A,\sigma}, Cd_{X,A,\sigma}C^{-1} = d^\dagger_{X,A,\sigma}, \\ Cd^\dagger_{X,B,\sigma}C^{-1} &= -d_{X,B,\sigma}, Cd_{X,B,\sigma}C^{-1} = -d^\dagger_{X,B,\sigma}, \\ C\hat{\phi}_X C^{-1} &= \hat{\phi}_X + \pi, CiC^{-1} = -i, \end{aligned} \tag{15}$$

where $C^2 = \mathcal{I}$. As compared to refs. 57,71, note that we have extended C to bosons such that it reverses the charge of the bosons and preserves the commutation relations.

Bogoliubov-de Gennes Hamiltonian

The Bloch Hamiltonian for static, homogenous Δ takes the form $H = \int \frac{dp}{2\pi} \Psi^\dagger(p) H(p) \Psi(p)$ where $\Psi(p) = (d_{A,\uparrow}(p), d_{B,\uparrow}(p), d^\dagger_{A,\downarrow}(-p), d^\dagger_{B,\downarrow}(-p))^T$. Clearly, in the absence of SSB, i.e. for $\Delta = 0$, $H(p)$ is block diagonal as illustrated schematically in Fig. 1. It is convenient to choose a different basis leading to Eq. (4). The winding represented in Fig. 1a), b) correspond to the parametric plot of eigenvalues of $D(p)$ at $t = 0.1t'$ and $\Delta = 0$ for a) and $\Delta = 0.1t'$ for panel b).

Parameters of the continuum field theory

The parameters in Eq. (8) are defined as follows in terms of the model parameters in Eq. (3):

$$\begin{aligned} K_s &= \frac{1}{1+\frac{\Delta^2}{8E_C t'\pi}}, \quad K_\rho = \frac{1}{\sqrt{(1-\frac{\Delta^2}{8E_C t'\pi})(1-\frac{\Delta^2}{8E_C t'\pi}+\frac{E_C}{4t'\pi})}}, \\ u_s &= t'a, \qquad u_\rho = u_s\sqrt{\frac{1-\frac{\Delta^2}{8E_C t'\pi}+\frac{E_C}{4t'\pi}}{1-\frac{\Delta^2}{8E_C t'\pi}}}, \\ G_s &= \frac{\Delta^2}{8\pi^2 E_C a}, \qquad M = \frac{2(t'-t)}{\pi a}. \end{aligned} \tag{16}$$

Note that these expressions are valid close to $t = t'$ and we generally assume $E_C \ll \sqrt{t^2+t'^2}$.

Luttinger parameters of the superconductor

To integrate out fermions, we expand the transformed Hamiltonian, obtained after the unitary transformation, in terms of $(\hat{\phi}_{X+1} - \hat{\phi}_X)$ up to second order and also rewrite it in the action formalism. The corresponding action is given by:

$$\begin{aligned} S = S_0(\phi) + S_0(d,\bar{d}) + \Delta S_1(\phi,d,\bar{d}) \\ + \Delta S_2(\phi,d,\bar{d}), \end{aligned} \tag{17}$$

where $d/\bar{d}$ represent Grassmann variables and ϕ represents the superconducting phase. The effective bosonic action is given by:

$$\begin{aligned} S_{\text{eff}}(\phi) = S_0(\phi) + \left\langle \Delta S_1(\bar{d}, d, \phi) \right\rangle \\ + \left\langle \Delta S_2(\bar{d}, d, \phi) \right\rangle \\ - \frac{1}{2}(\left\langle \Delta S_1^2(\bar{d}, d, \phi) \right\rangle - \left\langle \Delta S_1(\bar{d}, d, \phi) \right\rangle^2), \end{aligned} \tag{18}$$

where,

$$\langle . \rangle = \frac{1}{Z_0(\bar{d}, d, \phi)} \int \mathcal{D}\bar{d}\mathcal{D}d.e^{-S_0(\bar{d}, d)}. \tag{19}$$

The parameters entering the effective superconducting theory in $S_{\text{eff}}(\phi)$ given in Eq. (14) are related to the microscopic parameters as follows:

$$\begin{aligned} K_{\text{SC}} &= 2\sqrt{\frac{4\pi^2 E_{\text{C}} a}{vI}}, \\ u_{\text{SC}} &= 4\sqrt{\frac{vIE_{\text{C}} a}{4\pi^2}}, \\ v &= t' a, \\ I &= \frac{2\pi\delta^2 \cos(\theta)\text{EllipticE}\left(-\frac{2\sin(2\theta)}{\delta^2+1-\sin(2\theta)}\right)}{\sqrt{\delta^2+1-\sin(2\theta)}\left(\delta^2+1+\sin(2\theta)\right)}, \end{aligned} \tag{20}$$

where $\theta = \arctan(\frac{t}{t'})$ and $\delta = \frac{\Delta}{\sqrt{t^2+t'^2}}$. K_{SC} represents inverse superconducting stiffness. Further details are provided in supplementary note 4.

Data availability

The numerical data that support the findings of this study are available from Zenodo repository 10.5281/zenodo.11243225[72].

Code availability

The code used for numerical simulations is available from Zenodo repository 10.5281/zenodo.11243225[72].

Received: 17 November 2024; Accepted: 19 October 2025;
Published online: 04 November 2025

References

1. Landau, L. D. On the theory of phase transitions. i. *Zh. Eksp. Teor. Fiz.* **11**, 19 (1937).
2. Fernandes, R. M., Orth, P. P. & Schmalian, J. Intertwined vestigial order in quantum materials: Nematicity and beyond. *Annu. Rev. Condens. Matter Phys.* **10**, 133–154 (2019).
3. Svistunov, B. V., Babaev, E. S. & Prokof'ev, N. V. *Superfluid states of matter* (CRC Press, 2015).
4. Savary, L. & Balents, L. Quantum spin liquids: a review. *Rep. Prog. Phys.* **80**, 016502 (2016).
5. Wen, X. G. & Zee, A. Quantum disorder, duality, and fractional statistics in 2+1 dimensions. *Phys. Rev. Lett.* **62**, 1937–1940 (1989).
6. Sachdev, S. Quantum magnetism and criticality. *Nat. Phys.* **4**, 173–185 (2008).
7. Wang, C. & Senthil, T. Interacting fermionic topological insulators/superconductors in three dimensions. *Phys. Rev. B* **89**, 195124 (2014).
8. Wang, J. & You, Y.-Z. Symmetric mass generation. *Symmetry* **14**, 1475 (2022).
9. Chen, X., Gu, Z.-C., Liu, Z.-X. & Wen, X.-G. Symmetry protected topological orders and the group cohomology of their symmetry group. *Phys. Rev. B* **87**, 155114 (2013).
10. Senthil, T. Symmetry-protected topological phases of quantum matter. *Annu. Rev. Condens. Matter Phys.* **6**, 299–324 (2015).
11. Kitaev, A. On the classification of short-range entangled states http://scgp.stonybrook.edu/video_portal/video.php?id=2010 (2013).
12. Chen, X., Gu, Z.-C. & Wen, X.-G. Local unitary transformation, long-range quantum entanglement, wave function renormalization, and topological order. *Phys. Rev. B* **82**, 155138 (2010).
13. Qi, X.-L. & Zhang, S.-C. Topological insulators and superconductors. *Rev. Mod. Phys.* **83**, 1057–1110 (2011).
14. Haldane, F. D. M. Continuum dynamics of the 1-d Heisenberg antiferromagnet: Identification with the O(3) nonlinear sigma model. *Phys. Lett. A* **93**, 464–468 (1983).
15. Affleck, I., Kennedy, T., Lieb, E. H. & Tasaki, H. Rigorous results on valence-bond ground states in antiferromagnets. *Phys. Rev. Lett.* **59**, 799–802 (1987).
16. Fidkowski, L. & Kitaev, A. Topological phases of fermions in one dimension. *Phys. Rev. B* **83**, 075103 (2011).
17. Pollmann, F., Turner, A. M., Berg, E. & Oshikawa, M. Entanglement spectrum of a topological phase in one dimension. *Phys. Rev. B* **81**, 064439 (2010).
18. Turner, A. M., Pollmann, F. & Berg, E. Topological phases of one-dimensional fermions: An entanglement point of view. *Phys. Rev. B* **83**, 075102 (2011).
19. Pollmann, F. & Turner, A. M. Detection of symmetry-protected topological phases in one dimension. *Phys. Rev. B* **86**, 125441 (2012).
20. Gu, Z.-C. & Wen, X.-G. Symmetry-protected topological orders for interacting fermions: Fermionic topological nonlinear σ models and a special group supercohomology theory. *Phys. Rev. B* **90**, 115141 (2014).
21. Ryu, S., Schnyder, A. P., Furusaki, A. & Ludwig, A. W. Topological insulators and superconductors: tenfold way and dimensional hierarchy. *N. J. Phys.* **12**, 065010 (2010).
22. Kitaev, A. Periodic table for topological insulators and superconductors. In *AIP Conference Proceedings*, vol. 1134, 22–30 (American Institute of Physics, 2009). https://arxiv.org/abs/0901.2686.
23. Haegeman, J., Pérez-García, D., Cirac, I. & Schuch, N. Order parameter for symmetry-protected phases in one dimension. *Phys. Rev. Lett.* **109**, 050402 (2012).
24. Fidkowski, L. & Kitaev, A. Effects of interactions on the topological classification of free fermion systems. *Phys. Rev. B* **81**, 134509 (2010).
25. Lapa, M. F., Teo, J. C. Y. & Hughes, T. L. Interaction-enabled topological crystalline phases. *Phys. Rev. B* **93**, 115131 (2016).
26. Rachel, S. Interacting topological insulators: a review. *Rep. Prog. Phys.* **81**, 116501 (2018).
27. Ostrovsky, P. M., Gornyi, I. V. & Mirlin, A. D. Quantum criticality and minimal conductivity in graphene with long-range disorder. *Phys. Rev. Lett.* **98**, 256801 (2007).
28. Fu, L. & Kane, C. L. Topology, delocalization via average symmetry and the symplectic anderson transition. *Phys. Rev. Lett.* **109**, 246605 (2012).
29. König, E. J. et al. Half-integer quantum Hall effect of disordered Dirac fermions at a topological insulator surface. *Phys. Rev. B* **90**, 165435 (2014).
30. Ma, R. & Wang, C. Average symmetry-protected topological phases. *Phys. Rev. X* **13**, 031016 (2023).
31. Altland, A., Bagrets, D., Fritz, L., Kamenev, A. & Schmiedt, H. Quantum criticality of quasi-one-dimensional topological anderson insulators. *Phys. Rev. Lett.* **112**, 206602 (2014).
32. Altland, A., Bagrets, D. & Kamenev, A. Topology versus anderson localization: Nonperturbative solutions in one dimension. *Phys. Rev. B* **91**, 085429 (2015).
33. Grushin, A. G. Topological phases of amorphous matter. In *Low-Temperature Thermal and Vibrational Properties of Disordered Solids: A Half-Century of Universal "Anomalies" of Glasses*, 435–486 (World Scientific, 2023). https://www.worldscientific.com/worldscibooks/10.1142/q0371#t=aboutBook.

34. Ma, R., Zhang, J.-H., Bi, Z., Cheng, M. & Wang, C. Topological phases with average symmetries: the decohered, the disordered, and the intrinsic. *Phys. Rev. X* **15**, 021062 (2025).
35. Schnyder, A. P., Ryu, S., Furusaki, A. & Ludwig, A. W. W. Classification of topological insulators and superconductors in three spatial dimensions. *Phys. Rev. B* **78**, 195125 (2008).
36. Rampp, M. A., König, E. J. & Schmalian, J. Topologically enabled superconductivity. *Phys. Rev. Lett.* **129**, 077001 (2022).
37. Bollmann, S., Väyrynen, J. I. & König, E. J. Topological Kondo effect with spinful Majorana fermions. *Phys. Rev. B* **110**, 035136 (2024).
38. Else, D. V. Topological Goldstone phases of matter. *Phys. Rev. B* **104**, 115129 (2021).
39. Gurarie, V. Single-particle Green's functions and interacting topological insulators. *Phys. Rev. B* **83**, 085426 (2011).
40. You, Y.-Z. & Xu, C. Symmetry-protected topological states of interacting fermions and bosons. *Phys. Rev. B* **90**, 245120 (2014).
41. Defenu, N. et al. Long-range interacting quantum systems. *Rev. Mod. Phys.* **95**, 035002 (2023).
42. Ruderman, M. A. & Kittel, C. Indirect exchange coupling of nuclear magnetic moments by conduction electrons. *Phys. Rev.* **96**, 99–102 (1954).
43. Kasuya, T. A theory of metallic ferro-and antiferromagnetism on Zener's model. *Prog. Theor. Phys.* **16**, 45–57 (1956).
44. Yosida, K. Magnetic properties of Cu-Mn alloys. *Phys. Rev.* **106**, 893–898 (1957).
45. Su, W. P., Schrieffer, J. R. & Heeger, A. J. Soliton excitations in polyacetylene. *Phys. Rev. B* **22**, 2099–2111 (1980).
46. Ryu, S. & Hatsugai, Y. Entanglement entropy and the Berry phase in the solid state. *Phys. Rev. B* **73**, 245115 (2006).
47. Li, G., König, E. J. & Väyrynen, J. I. Topological symplectic Kondo effect. *Phys. Rev. B* **107**, L201401 (2023).
48. Knapp, C., Väyrynen, J. I. & Lutchyn, R. M. Number-conserving analysis of measurement-based braiding with Majorana zero modes. *Phys. Rev. B* **101**, 125108 (2020).
49. Shi, Z., Brouwer, P. W., Flensberg, K., Glazman, L. I. & von Oppen, F. Long-distance coherence of Majorana wires. *Phys. Rev. B* **101**, 241414 (2020).
50. Giorgadze, I., Huang, H., Gaines, J., König, E. J. & Väyrynen, J. I. Characterizing maximally many-body entangled fermionic states by using *m*-body density matrix. *Quantum* **9**, 1778 (2025).
51. Turner, A. M., Vishwanath, A. & Head, C. O. Beyond band insulators: topology of semimetals and interacting phases. *Topol. Insul.* **6**, 293 (2013).
52. Callan, C. G. Broken scale invariance in scalar field theory. *Phys. Rev. D.* **2**, 1541–1547 (1970).
53. Giamarchi, T.*Quantum physics in one dimension*. International series of monographs on physics (Clarendon Press, Oxford, 2004). https://cds.cern.ch/record/743140.
54. Keselman, A. & Berg, E. Gapless symmetry-protected topological phase of fermions in one dimension. *Phys. Rev. B* **91**, 235309 (2015).
55. Kosterlitz, J. M. & Thouless, D. J. Ordering, metastability and phase transitions in two-dimensional systems. In *Basic Notions Of Condensed Matter Physics*, 493–515 (CRC Press, 2018). https://iopscience.iop.org/article/10.1088/0022-3719/6/7/010.
56. Hauschild, J. & Pollmann, F. Efficient numerical simulations with tensor networks: Tensor network python (tenpy). *SciPost Physics Lecture Notes* 005 https://www.scipost.org/10.21468/SciPostPhysLectNotes.5 (2018).
57. Zirnbauer, M. R. Particle-hole symmetries in condensed matter. *J. Math. Phys.* **62**, 021101 (2021).
58. Chen, X., Gu, Z.-C. & Wen, X.-G. Complete classification of one-dimensional gapped quantum phases in interacting spin systems. *Phys. Rev. B* **84**, 235128 (2011).
59. Benthien, H., Essler, F. & Grage, A. Quantum phase transition in the one-dimensional extended Peierls-Hubbard model. *Phys. Rev. B* **73**, 085105 (2006).
60. Manmana, S. R., Essin, A. M., Noack, R. M. & Gurarie, V. Topological invariants and interacting one-dimensional fermionic systems. *Phys. Rev. B* **86**, 205119 (2012).
61. Sirker, J., Maiti, M., Konstantinidis, N. & Sedlmayr, N. Boundary fidelity and entanglement in the symmetry protected topological phase of the SSH model. *J. Stat. Mech.: Theory Exp.* **2014**, P10032 (2014).
62. Yahyavi, M., Saleem, L. & Hetényi, B. Variational study of the interacting, spinless Su–Schrieffer–Heeger model. *J. Phys.: Condens. Matter* **30**, 8pp (2018).
63. Nersesyan, A. A. Phase diagram of an interacting staggered Su-Schrieffer-Heeger two-chain ladder close to a quantum critical point. *Phys. Rev. B* **102**, 045108 (2020).
64. Matveeva, P., Gutman, D. & Carr, S. T. Weakly interacting one-dimensional topological insulators: A bosonization approach. *Phys. Rev. B* **109**, 165436 (2024).
65. Padhan, A., Mondal, S., Vishveshwara, S. & Mishra, T. Interacting bosons on a Su-Schrieffer-Heeger ladder: Topological phases and Thouless pumping. *Phys. Rev. B* **109**, 085120 (2024).
66. Wagner, N. et al. Mott insulators with boundary zeros. *Nat. Commun.* **14**, 7531 (2023).
67. Soldini, M. O. et al. Interacting topological quantum chemistry of Mott atomic limits. *Phys. Rev. B* **107**, 245145 (2023).
68. Manning-Coe, D. & Bradlyn, B. Ground state stability, symmetry, and degeneracy in Mott insulators with long-range interactions. *Phys. Rev. B* **108**, 165136 (2023).
69. Setty, C. et al. Electronic properties, correlated topology, and Green's function zeros. *Phys. Rev. Res.* **6**, 033235 (2024).
70. Bollmann, S., Setty, C., Seifert, U. F. & König, E. J. Topological green's function zeros in an exactly solved model and beyond. *Phys. Rev. Lett.* **133**, 136504 (2024).
71. Verresen, R., Moessner, R. & Pollmann, F. One-dimensional symmetry protected topological phases and their transitions. *Phys. Rev. B* **96**, 165124 (2017).
72. Tiwari, D., Bollmann, S., Paeckel, S. & J. König, E. Supporting data and code https://zenodo.org/uploads/11243225 (2024).

Acknowledgements

It is a pleasure to thank Sam Carr, Frank Pollmann, Ruben Verresen, Johannes Hauschild, Martin R. Zirnbauer, Yuval Oreg for useful input and to thank Thomas Köhler for collaboration on a related project. DT thanks Kirill Parshukov, Nikolaos Parthenios, and Raffaele Mazzilli for useful discussions. We would also like to thank the reviewers for their valuable input, which helped us in improving our manuscript during the peer review process. Support for this research was provided by the Office of the Vice Chancellor for Research and Graduate Education at the University of Wisconsin-Madison with funding from the Wisconsin Alumni Research Foundation. This research was supported in part by a grant NSF PHY-2309135 to the Kavli Institute for Theoretical Physics (KITP). DT thanks Max Planck Institute for Solid State Research for the IMPRS fellowship. SP acknowledges support from the Munich Center for Quantum Science and Technology. EJK acknowledges hospitality by the KITP.

Author contributions

E.J.K. conceived and supervised the project. D.T. performed all calculations under the guidance of S.B., S.P., E.J.K. All co-authors analyzed the results and wrote the manuscript.

Funding

Open Access funding enabled and organized by Projekt DEAL.

Competing interests
The authors declare no competing interests.

Additional information
Supplementary information The online version contains supplementary material available at https://doi.org/10.1038/s42005-025-02385-7.

Correspondence and requests for materials should be addressed to Dhruv Tiwari.

Peer review information *Communications Physics* thanks Lorenzo Maffi and the other anonymous reviewer(s) for their contribution to the peer review of this work. A peer review file is available.